RSC Advances

ROYAL SOCIETY OF CHEMISTRY

www.rsc.org/advances

Controlling of the Oxidation Level of Graphene Oxide for High Efficient Polymer Solar Cells

Rui Wu[a], Lie Chen[a,b], Liqiang Huang[a], Yiwang Chen*[,a,b]

[a] *College of Chemistry/Institute of Polymers, Nanchang University, 999 Xuefu Avenue, Nanchang 330031, China*

[b] *Jiangxi Provincial Key Laboratory of New Energy Chemistry, Nanchang University, 999 Xuefu Avenue, Nanchang 330031, China*

The graphene oxides (GOs) have been used as an interfacial layer for fabricating more stable organic solar cells (OSCs). However, influence of oxidation degree of GOs on its optoelectronic properties has been ignored. In this article, a series of GOs with different degrees of oxidation were successfully synthesized, by controlling the amount of oxidant $KMnO_4$ during the oxidation process of graphite. With oxidation level increasing, more oxygenated functional groups were attached to the carbon basal plane and more defects were introduced into the GOs sheets, resulting in an increased work function (WF) and decreased conductivity. Meanwhile, the film-forming property of GOs was improved with oxidation level increasing, which is attributed to the adequate exfoliation of GOs sheets. After carefully controlling oxidized level of GOs, the OSCs with GOs as hole transport layer (HTL) show a comparable efficiency value of 3.0% to that with poly(3,4-ethylenedioxythiophene):poly(styrenesulfonate) (PEDOT:PSS) (3.2%), originating from the good film-forming property, appropriate work function and high conductivity.

Keywords: graphene oxide, oxidation level, work function, morphology, conductivity, organic solar cell

Introduction

Organic solar cells (OSCs) represent an exciting class of renewable energy technology. They are under intensive investigation in both academia and industry due to their great potential to enable mass manufacture of flexible and low-cost devices through roll-to-roll techniques.[1] Power conversion efficiencies (PCE) of OSCs have increased continuously over the last few years. The PCE of OSCs has exceeded 10% for the single cell[2] and 11% for the tandem cell.[3] In bulk heterojunction OSC devices, the interface between the active layer and the electrodes play an important role for its high efficiency and stability. [4] In order to improve the efficiency and stability of OSCs, hole transport layer (HTL) and electron transport layer (ETL) materials are used at the anode interface and cathode interface, to minimize carrier recombination loss and current leakage at the interface between electrodes and semiconducting materials.[5]

For the anode interface, PEDOT:PSS is the most commonly used HTL material. Several problems of the PEDOT:PSS include high acidity and hygroscopic properties, resulting in poor long-term stability of OSCs. Li *et al.*[6] first reported that graphene oxide (GO) can be used as a hole transport layer material for fabricating more stable OSCs, potentially replacing PEDOT:PSS. GO is a graphene sheet functionalized with oxygen groups including epoxy, hydroxyl, carboxyl and carbonyl.[7] The availability of reactive carboxyl and epoxy/hydroxyl of GO sheet facilitates further functionalization of GO, permitting tunability of optoelectronic properties.[8] Besides, GO can be processed in solution at large scale with low-cost, particularly attractive for massive applications. Due to the advantages of GO, it has been a promising interface modification material for OSCs. Over the past few years, there has been significant progress in the application of GO in OSCs.[9] Both pristine GO and its derivatives as interfacial layer of OSCs generally need to change the work function through functionalized or doped with molecules, to favor an energy alignment in the devices.[10] Stratakis *et al.*[11] demonstrated that GO's work function can be tuned by treated with ultraviolet laser and chlorine gas. Similarly, sulfated[12] and fluorine-functionalized GO[13] with increased work function were also used as the HTL in OSCs. Moreover, the work function of GO can be effectively reduced, triggering its use as ETL.[14] Besides, the use of conductive fillers to improve the conductivity of GO has also been investigated.[15]

Actually, GOs synthesized by different methods and conditions have different degrees of oxidation. However, in the recent years, most efforts mainly focus on how to improve the performance of the GO by functionalized or doped with other molecules, but the modulation of oxidation degree of GO on its optoelectronic properties has been ignored. Clearly, it's a critical issue for the further application of GO in OSCs. In this study, a series of graphene oxides (GOs) with different degrees of oxidation were successfully synthesized, by carefully controlling the amount of oxidant $KMnO_4$ during the oxidation process of graphite, and the effect of GO's oxidized level on its optoelectronic properties has been systematically studied.

Experimental

Preparation of Graphene Oxide (GO).

GOs were prepared by oxidation of graphite powder according to a modified Hummer's method.[16] Briefly, Graphite (1.0 g) was added to concentrated sulfuric acid (25 ml) under stirring at room temperature, then sodium nitrate (0.5 g) was added, and the mixture was cooled to 0°C. Under violent agitation, potassium permanganate (0.5 g, 50 wt%) was added slowly to keep the temperature of the reaction system lower than 20°C. Then, the suspension was transferred to a 35°C water bath and vigorous stirred for about 1.0 h. Subsequently, 50 ml of water was added, and the solution was stirred for 15 min at 90°C. Additional 180 ml of water was added and followed by a slow addition of 5 ml of H_2O_2 (3%), turning the color of the suspension from dark brown to yellow. The solution was filtered and washed with 1:10 HCl aqueous solution (100 ml) to remove metal ions followed by washing with 100 ml of water to remove the acid. In the end, it was purified by dialysis for several days to remove the remaining metal species. Similar process was followed for GOs with different degrees of oxidation by adding 0.5 g (50 wt%), 1 g (100 wt%), 4 g (400 wt%) and 6 g (600 wt%) of $KMnO_4$.

Characterization

The resultant GOs with different degrees of oxidation were investigated by Raman spectrum (LabRam-1B), Fourier transform infrared spectroscopy (FT- IR Prestige-21), X-ray photoelectron spectroscopy (Thermo-VG Scientific ESCALAB 250), Wide-angle X-ray diffraction (Bruker D-8). Transmittance spectra were analyzed by UV−vis spectroscopy (PerkinElmer Lambda 750). The morphology of GOs was characterized by using scanning electron microscopy (QuanTA-200F environmental scanning electron microscope), atomic force microscopy (Agilent 5500) and transmission electron microscopy (JEOL, JEM-2100F). Ultraviolet photoelectron spectroscopy (UPS) was carried out by the AXISULTRA DLD spectrometer (Kratos Analytical Ltd.). The current-voltage characteristics of devices under illumination were tested by a Keithley 2400 Source Meter. The light intensity was 100 Mw/cm^2.

Device fabrication:

All the devices were fabricated with the structure of ITO/HTL/P3HT:PCBM/LiF/Al. The ITO substrates were cleaned by ultrasonication in soap water, deionized water, acetone and isopropanol.

After drying ITO substrates and treating the surface with UV ozone for 15 minutes, the interface layers of the devices were deposited on the ITO substrates using the following spin-coating conditions, respectively. The PEDOT:PSS layer was spin-coated from the solution at 4000 rpm for 60 s, followed by heating at 140 °C for 15 min. The GO layers were spin-coated from its solution in water (0.5 mg/ml) at 2000 rpm for 60 s, followed by heating at 140 °C for 10 min. The active layer was sequentially spin-coated from the solution of P3HT/PCBM =1/1 in o-dichlorobenzene (20 mg/ml) at 800 rpm for 30 s, followed by thermal annealing at 150 °C for 10 min. After spin-coating of the organic layers, the devices were transferred into a vacuum chamber for thermal deposition of LiF (0.7 nm) and Al (100 nm) at a pressure of 10^{-7} Torr. The area of each device was 0.04 cm^2, as determined by the overlap of the ITO and Al.

Results and discussion

We synthesized four GOs with different degrees of oxidation, which were named GO (50 wt% $KMnO_4$), GO (100 wt% $KMnO_4$), GO (400 wt% $KMnO_4$) and GO (600 wt% $KMnO_4$), according to the different additive amount of oxidant $KMnO_4$. **Figure 1a** shows the X-ray photoelectron spectroscopy (XPS) survey spectra of four GOs. Two intense characteristic peaks of C and O are observed. **Figure 1b** shows the high-resolution XPS C1s spectra. With the increase in the amount of oxidant $KMnO_4$, the oxidation level of GO increases, as evidenced by the decrease of C/O. [17] The resultant Fourier transform infrared spectroscopy (FT-IR) of the prepared GOs with different degrees of oxidation is shown in **Figure 2a**. The band at about 1579 cm^{-1} is due to the presence of C–C stretching in graphitic domains. With increases in oxidation level, the FT-IR spectrum reveals more oxygenated functional groups, including C-OH (~1399 cm^{-1}), C-O-C (~1249 cm^{-1}), C=O (~1727 cm^{-1}), C-O (~1049 cm^{-1}).[18] It indicates that more oxygenated functional groups were attached to the carbon basal plane. Then, GOs were analyzed by Raman spectra, as shown in **Figure 2b**. Two prominent peaks were observed in the GO spectra, which correspond to D-peak and G-peak. The D peak exhibits the defect nature of GO, while the G peak is the characteristic peak of the sp^2 carbon atom vibration. And the ratio (I_D/I_G) of the intensity of D peak (I_D) and G peak (I_G) increased with the increase of oxidant level. The reason is that there was more defect in the GO sheet with the addition of oxygenated functional groups. **Figure 3** shows the X-ray diffraction (XRD) patterns of the GOs with different degrees of oxidation. The XRD pattern of the original graphite shows a diffraction peak at 2θ=26.5° associated to an interlayer spacing of about 3.36 Å. However, with increasing degrees of oxidation, the intensity of this peak starts to decrease, and finally, disappear at the higher oxidation levels. Meanwhile, it also can be observed appearance of a new peak at a lower angle, corresponding to the diffraction pattern of GOs, starts to appear. The interlayer spacing (d) of the GO increases from 6.81 Å to 7.90 Å as oxidant level increases (**Table S1**), due to the addition of oxygenated functional groups weakening the π-π stacking between GO sheets.[19]

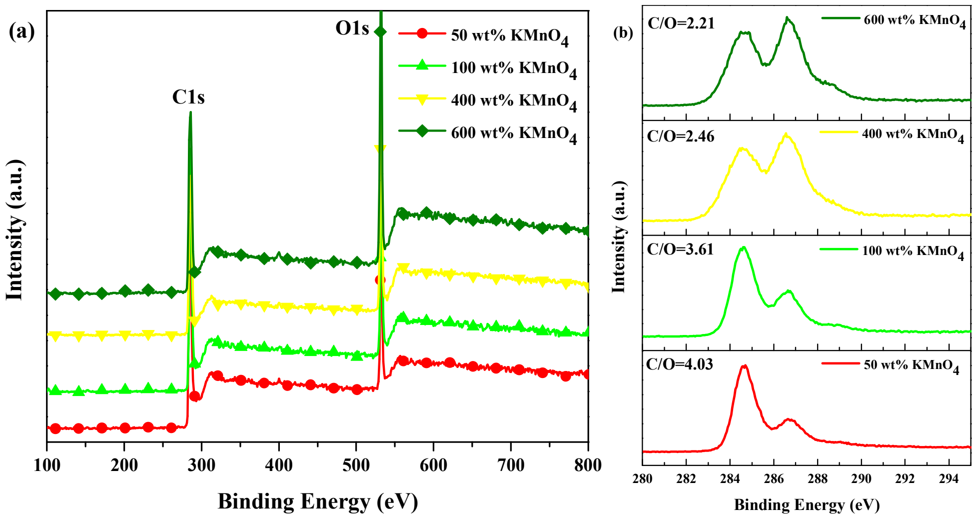

Figure 1. (a) XPS survey spectra of GOs with different degrees of oxidation (50 wt% KMnO$_4$, 100 wt% KMnO$_4$, 400 wt% KMnO$_4$ and 600 wt% KMnO$_4$ represent the input of KMnO$_4$ corresponding to 1 g graphite). (b) High-resolution XPS C1s spectra of GOs with different degrees of oxidation (C/O represents the ratio of C and O in GOs with different degrees of oxidation).

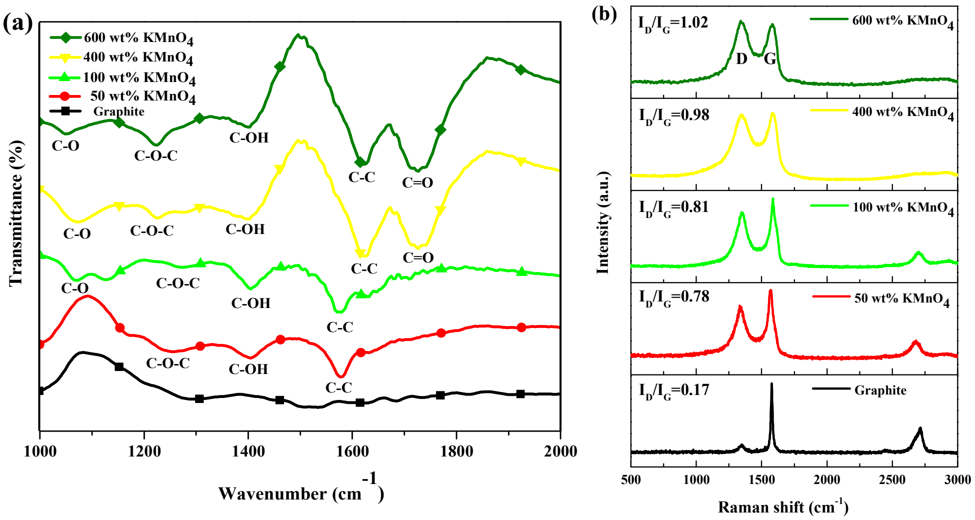

Figure 2. (a) Fourier transforms infrared spectra and (b) Raman spectra of GOs with different degrees of oxidation such as 50 wt% $KMnO_4$, 100 wt% $KMnO_4$, 400 wt% $KMnO_4$ and 600 wt% $KMnO_4$.

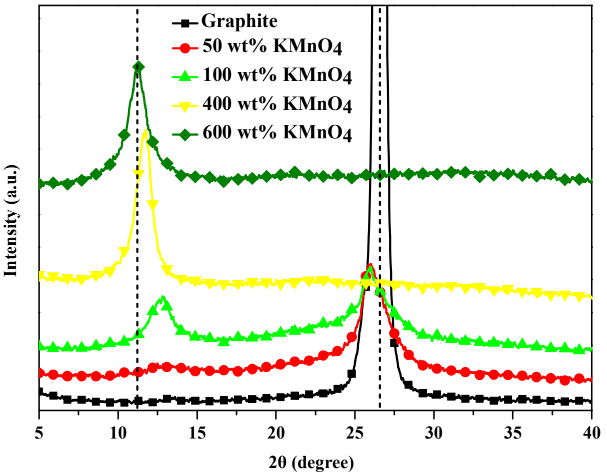

Figure 3. X-ray diffraction patterns of GOs with different degrees of oxidation such as 50 wt% $KMnO_4$, 100 wt% $KMnO_4$, 400 wt% $KMnO_4$ and 600 wt% $KMnO_4$.

Interfacial morphology and its contact with the active layer are crucial for OSCs performance, thus the effect of the degree of oxidation on the morphology and surface wettability of the GO has been investigated. Surface contact angle of the GOs with different degrees of oxidation has been shown in **Figure S1**. Attaching the hydrophilic oxygenated functional groups on the graphene results in a decrease in the surface contact angle of GOs, especially in the GO with high degree of oxidation. However, compared to the surface contact angle of PEDOT:PSS (16°, **Figure S1e**), these GOs still remain a moderate surface wettability with a surface contact angle of 60~70°, which can improve the interface compatibility of the active layer and HTL in OSCs. The atomic force microscope (AFM) was then used to analyze the surface morphology of GOs with different degrees of oxidation. The results show that all samples of GOs have similar value of roughness (**Figure S2**). However, the difference in the morphology caused by the degrees of oxidation can be clearly detected by transmission electron microscope (TEM), as shown in **Figure 4**. It is obvious that all the samples of GOs have a lamellar morphology. GO (50 wt% $KMnO_4$, **Figure 4a**) shows a serious aggregation, due to the partially oxidized graphene oxide leading to an unsuccessful exfoliation. With degrees of oxidation increasing, the dispersion of GOs is improved greatly, and the transparent GO sheet can be obviously observed, implying that the adequate exfoliation of samples. These observation is also correlated with the scanning electron microscopy (SEM) images in **Figure S3**. Compared with GO with low degree of oxidation containing closely aggregation graphene oxide (**Figure S3a)**, GO (100 wt% $KMnO_4$ **Figure S3b**), GO (400 wt% $KMnO_4$ **Figure S3c**) and GO (600 wt% $KMnO_4$ **Figure S3d**) show much more smooth surface, in favor of the process of following active layer and forming of stable interface.

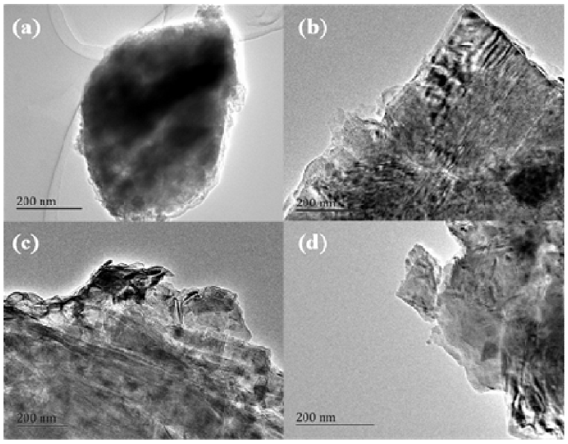

Figure 4. Transmission electron microscopy images of GOs with different degrees of oxidation. (a) 50 wt% $KMnO_4$, (b) 100 wt% $KMnO_4$, (c) 400 wt% $KMnO_4$ and (d) 600 wt% $KMnO_4$.

Prior to employ GOs with different degrees of oxidation as the hole transport layers in OSCs, its work functions were measured with ultraviolet photoelectron spectroscopy (UPS) (**Figure 5a**). The work functions of GOs coated on ITO glass with different degrees of oxidation can be calculated from the following equation.[20]

$$\mathrm{WF} = hv - E_{\mathrm{F}} + E_{\mathrm{cutoff}}$$

Where hv is the He(I) excitation energy equal to 21.2 eV, E_{F} is the Fermi level, and E_{cutoff} is the high-binding energy cutoff. The work functions of GOs oxided from 50 wt%, 100 wt%, 400 wt% and 600 wt% $KMnO_4$ were 4.8 eV, 4.9 eV, 5.1 eV and 5.1 eV, respectively. These values were higher than typical value (4.6 eV) obtained for pristine graphene. The higher values for GOs are due to the surface $C^{\delta+}$-$O^{\delta-}$ dipoles. The induced polar character of $C^{\delta+}$-$O^{\delta-}$ bonds is responsible for the downward shift of the Fermi level of GOs, and the subsequent increase in the work functions from 4.6 eV to 5.1 eV. With increase of oxygenated functional groups in the base plane of carbon, intensity of the surface $C^{\delta+}$-$O^{\delta-}$ dipoles enhance, resulting in the further rise of GOs work functions. Obviously, the WF of GOs oxided from 400 wt% and 600 wt% $KMnO_4$ matches the HOMO level of P3HT better (5.1 eV vs. 5.2 eV),[21] as shown in **Figure 5b**, thus the improved energy alignment is preferable to lower the Schottky barrier and form an ohmic contact at the ITO/active layer interface for charge extraction and collection.[22] The existence of the oxidized groups is expected to impact great on the conductivity of the GO, so the conductivity of the GOs layers with different degrees of oxidation was also evaluated with the device structure of ITO/GO/Al (**Figure 6a**). As respected, due to the growth of interlayer spacing (**Table S1**) and increase of GOs sheet defect (**Figure 2b**), the conductivity of GOs layers declines with the oxidation level increasing.

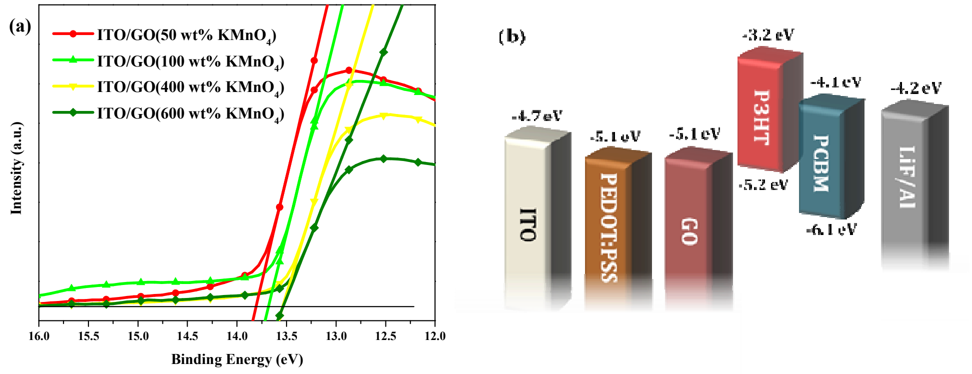

Figure 5. (a) Photoemission cutoff obtained via UPS for GOs with different degrees of oxidation. (b) The energy levels of all materials used in OSC cells.

To determine the performance of GOs with different degrees of oxidation as hole transport layers in OSCs, the OSC devices with the configuration of ITO/HTL/P3HT:PCBM(200 nm)/LiF(0.7 nm)/Al(100 nm) were fabricated (**Figure 6b**). Prior to it, the transmittance of GOs was investigated. **Figure S4** shows that all samples of GOs have favorable transmittance (> 80%), indicating that GOs can be used as HTL material. **Figure 6c** shows the illuminated current density−voltage ($J-V$) curves of the P3HT:PCBM-based OSCs devices with GOs and PEDOT:PSS as the HTL. The detailed photovoltaic characteristics are summarized in **Table 1**. The device with PEDOT:PSS HTL exhibits an averaged open-circuit voltage (V_{OC}) of 0.60 V, short-circuit current density (J_{SC}) of 8.32 mA/cm^2, fill factor (FF) of 0.604 and PCE of 3.1%, which is consistent with the reported value.[23] While, the device with GO (400 wt% $KMnO_4$) exhibits an averaged V_{OC} of 0.56 V, J_{SC} of 7.71 mA/cm^2, and FF of 0.636, leading to a PCE of 2.7%, and the best efficiency value (3.0%) of device with GO (400 wt% $KMnO_4$) HTL is comparable to that with PEDOT:PSS (3.2%). Comparing the performance of four GOs as HTLs, a clear trend of the power conversion efficiency with increasing oxidation level can be observed. For the first three GOs (50 wt% $KMnO_4$, 100 wt% $KMnO_4$ and 400 wt% $KMnO_4$), with increase in oxidation level, the average V_{OC} increase from 0.34 V to 0.56 V and the FF increase from 0.334 to 0.636, yielding the PCE from 0.9% to 2.7%. The enhanced V_{OC} with increasing of oxidation level can be attributed to gradually increased work functions of the GOs. Obviously, the 5.1 eV of GO (400 wt% $KMnO_4$) is almost equal to the HOMO level of P3HT (5.2 eV), leading to the largest V_{OC} (0.56 V). At the same time, the much more homogeneous dispersion and smoother surface of GO sheets (400 wt% $KMnO_4$) induces the improved FF, as depicted by SEM and TEM observation. However, when the amount of $KMnO_4$ increases to 600 wt%, the PCE together with all of the parameters of the device with GO (600 wt% $KMnO_4$) drop obviously, probably owing to its significant decrease of conductivity (**Figure 6a**). From the results we can see that careful control of the oxidation degree of GO can fine-tune the optoelectronic and film-forming properties, such as work function, conductivity and morphology, consequently leading to a satisfied device performance.

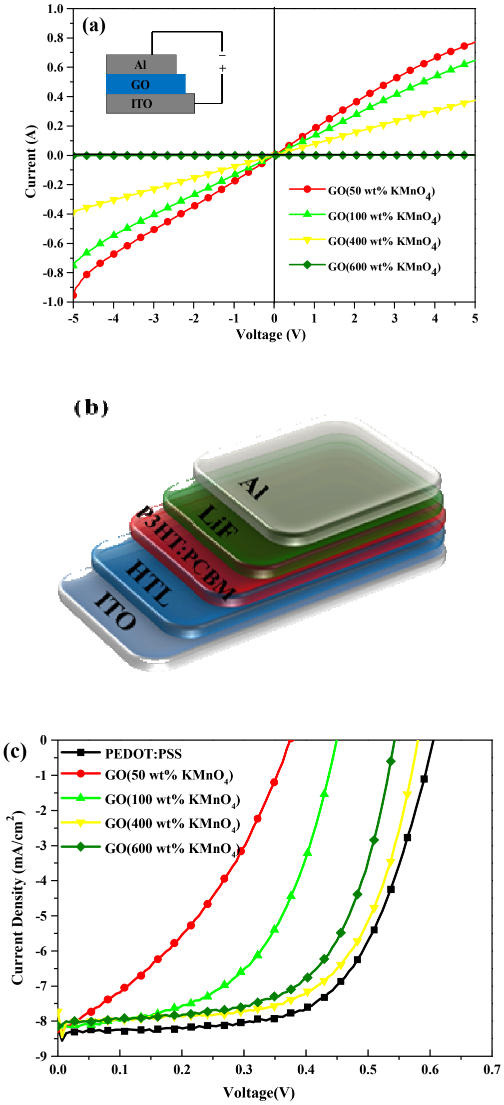

Figure 6. (a) *I*-*V* characteristics of GOs with different degrees of oxidation. (The inset represents the structure of device). With increases in oxidation level, conductivity of GOs with different degrees of oxidation decreases. (b) The structure of OSCs device. (c) *J*−*V* characteristics of P3HT:PCBM photovoltaic devices with different HTLs.

Table 1. Summary of the photovoltaic parameters of the fabricated OSCs[a].

HTL	J_{SC} [mA/cm ^{2}]	*Voc* [V]	FF[%]	PCE[%]
PEDOT:PSS	8.32±0.22	0.60±0.01	60.4±2.8	3.1±0.1(3.2)[b]
GO(50 wt% $KMnO_4$)	7.93±0.36	0.34±0.02	33.4±3.0	0.9±0.1(1.1)[b]
GO(100 wt%$KMnO_4$)	7.69±0.35	0.41±0.02	52.2±3.7	1.7±0.1(2.0)[b]
GO(400 wt%$KMnO_4$)	7.71±0.22	0.56±0.01	63.6±2.7	2.7±0.2(3.0)[b]
GO(600 wt%$KMnO_4$)	7.67±0.34	0.54±0.01	61.8±1.8	2.5±0.1(2.7)[b]

[a] Key: The structure of OSCs is ITO/HTL/P3HT:PCBM/LiF/Al. All values represent average from fourteen devices on a single chip. [b] The best device PCE.

Conclusions

In conclusion, a series of GOs with different degrees of oxidation have been successfully prepared, and the effect of GOs oxidized levels on its optoelectronic properties has also been systematically studied. With oxidation level increasing, more oxygenated functional groups were attached to the carbon basal plane and more defect were introduced into the GOs sheets, resulting in a increasing work function (from 4.8 eV to 5.1 eV) and decreasing conductivity. Meanwhile, the film-forming property was improved with increasing oxidation level, which is attributed to the more adequately exfoliation of GOs sheets. Due to its good film-forming property, appropriate work function and high enough conductivity, the OSCs device with the GO (400 wt% $KMnO_4$) as the HTL show the best PCE (3.0%), which is comparable with the PEDOT:PSS device (3.2%). In view of the significant effect of oxidized level on GO optoelectronic properties including film-forming property, work function and conductivity, this work indicates that controlling oxidized level plays a key role in achieving high performance OSC with GO HTL, and it would promote the further study and application of GO in OSCs.

Acknowledgement

This work was financially supported by the National Science Fund for Distinguished Young Scholars (51425304), National Natural Science Foundation of China (51273088, 51263016 and 51473075), and National Basic Research Program of China (973 Program 2014CB260409).

References

[1] Hu, X.; Chen, L.; Zhang, Y.; Hu, Q.; Yang, J.; Chen, Y. *Chem. Mater.* **2014,** *26* (21), 6293-6302.
[2] Chen, J. D.; Cui, C.; Li, Y. Q.; Zhou, L.; Ou, Q. D.; Li, C.; Li, Y.; Tang, J. X. *Adv. Mater.* **2014**.

DOI: 10.1002/adma.201404535.

[3] Chen, C. C.; Chang, W. H.; Yoshimura, K.; Ohya, K.; You, J.; Gao, J.; Hong, Z.; Yang, Y. *Adv. Mater.* **2014,** *26* (32), 5670-7.

[4] Yip, H.-L.; Jen, A. K. Y. *Energy Environ. Sci.* **2012,** *5* (3), 5994.

[5] Po, R.; Carbonera, C.; Bernardi, A.; Camaioni, N. *Energy Environ. Sci.* **2011,** *4* (2), 285.

[6] S, S. Li.; K, H. Tu.; C, C. Lin.; C, W. Chen.; M, Chhowalla. *ACS Nano*. **2010**, 4, 3169–3174.

[7] Gao, Y.; Yip, H. L.; Chen, K. S.; O'Malley, K. M.; Acton, O.; Sun, Y.; Ting, G.; Chen, H.; Jen, A. K. *Adv. Mater.* **2011,** *23* (16), 1903-8.

[8] Liu, J.; Durstock, M.; Dai, L. *Energy Environ. Sci.* **2014,** *7* (4), 1297.

[9] (a) Wang, D. H.; Kim, J. K.; Seo, J. H.; Park, I.; Hong, B. H.; Park, J. H.; Heeger, A. J. *Angew. Chem. Int. Ed.* **2013,** *52* (10), 2874-80; (b) Gao, Y.; Yip, H.-L.; Hau, S. K.; O'Malley, K. M.; Cho, N. C.; Chen, H.; Jen, A. K. Y. *Appl. Phys. Lett.* **2010,** *97* (20), 203306.

[10] (a) Yang, D.; Zhou, L.; Chen, L.; Zhao, B.; Zhang, J.; Li, C. *Chem. Commun.***2012,** *48* (65), 8078-80; (b) Yang, D.; Zhou, L.; Yu, W.; Zhang, J.; Li, C. *Adv. Energy Mater.* **2014,** *4* (15). DOI: 10.1002/aenm.201400591.

[11] Stratakis, E.; Savva, K.; Konios, D.; Petridis, C.; Kymakis, E. *Nanoscale* **2014,** *6* (12), 6925-31.

[12] Liu, J.; Xue, Y.; Dai, L. *J. Phys. Chem. Lett.* **2012,** *3* (14), 1928-1933.

[13] Kim, S. H.; Lee, C. H.; Yun, J. M.; Noh, Y. J.; Kim, S. S.; Lee, S.; Jo, S. M.; Joh, H. I.; Na, S. I. *Nanoscale* **2014,** *6* (13), 7183-7.

[14] Liu, J.; Xue, Y.; Gao, Y.; Yu, D.; Durstock, M.; Dai, L. *Adv. Mater.* **2012,** *24* (17), 2228-33.

[15] (a) Kim, J.; Tung, V. C.; Huang, J. *Adv. Energy Mater.* **2011,** *1* (6), 1052-1057; (b) Yin, B.; Liu, Q.; Yang, L.; Wu, X.; Liu, Z.; Hua, Y.; Yin, S.; Chen, Y. *J. Nanosci. Nanotechnol.* **2010,** *10* (3), 1934-1938.

[16] Xu,Y.;Zhao,L.;Bai,H.;Hong,W.;Li,Ch.;Shi,G. *J. Am. Chem. Soc.***2009**,131,13490

[17] C.K. Chua, M. Pumera. *Chem.Soc.Rev.* **2014**,43, 291-312.

[18] Krishnamoorthy, K.; Veerapandian, M.; Yun, K.; Kim, S. J. *Carbon* **2013,** *53*, 38-49.

[19] Thangavel, S.; Venugopal, G. *Powder Technol.* **2014,** *257*, 141-148.

[20] Ishii,H.; Sugiyama,K.; Ito,E.; Seki,K. *Adv. Mater.***1999**,11 (8),605-625

[21] Ji, T.; Tan, L.; Chen, Y. *Phys. Chem. Chem. Phys.***2014**. DOI: 10.1039/c4cp04965a

[22] Duan, C.; Zhang, K.; Zhong, C.; Huang, F.; Cao, Y. *Chem. Soc. Rev.* **2013,** *42* (23), 9071-104.

[23] Liu, X.; Kim, H.; Guo, L. J. *Org. Electron.* **2013,** *14* (2), 591-598.

Entry for the Table of Contents

Controlling of the Oxidation Level of Graphene Oxide for High Efficient Polymer Solar Cells

Rui Wu; Lie Chen; Liqiang Huang; Yiwang Chen*

Achieving high efficient polymer solar cells by controlling of the oxidation level of graphene oxide.

Graphical abstract